NUMERICAL STUDY OF MIXED CONVECTION HEAT TRANSFER THROUGH DOUBLE SQUARE CAVITY CONNECTED WITH EACH OTHER

Zainab K. Radhi
Mechanical Department- College of Engineering
University of Basrah

ABSTRACT

A numerical analysis is carried out to study the performance of mixed convection in a two square cavity connected one with other using finite element method with software package (FlexPDE). An external fluid flow enters the first cavity through an opening, fixed in the left vertical wall of the first cavity then passes through a second cavity and exits from other opening in the right vertical wall of the second cavity. The boundary conditions of the connected walls between the two cavities are maintained at a constant temperature (isothermal) while the other walls are adiabatic. In the present study streamlines, isotherms, average temperature and average Nusselt number of the heated walls are reported for a range of Richardson number $0 \leq Ri \leq 10$, Reynolds number $50 \leq Re \leq 200$, aspect ratio of heated walls, $0.1 \leq H_o \leq 0.9$ and different exit port positions H_{o1}= 0.1, 0.5 and 0.9 for a constant position of inlet port Hi=0.2 while Prandtl number is taken as Pr=0.71. The results of streamlines, isotherms, average Nusselt number and average temperature are compared with available result and excellent agreement has been achieved. The numerical results indicate that the rate of heat transfer is significantly depends on the rate of height of the heated walls (H_o), (Re) and (Ri) also the results show that the location of the exit port do not has important effects on the rate of heat transfer and with increasing Reynolds and Richardson numbers the convection heat transfer becomes predominant over the conduction heat transfer.

KEYWARDS: Heat Transfer, Laminar Flow, Mixed convection, Two Square Cavities Connected With Each Other.

دراسة عددية لعملية انتقال الحرارة بالحمل المختلط خلال فجوتين مربعتين مرتبطتين مع بعضهما

زينب كريم راضي
قسم الميكانيك-كلية الهندسة-جامعة البصرة

الخلاصة:

التحليل العددي بطريقة العناصر المحددة باستخدام الحقيبة البرمجية (FlexPDE) اجري لدراسة أداء مسألة انتقال الحرارة بالحمل المختلط داخل فجوتين مربعتين مرتبطتين مع بعضهما. الجريان الخارجي يدخل إلـى الفجوة الأولى من خلال فتحة مثبتة على الجدار الأيسر للفجوة الأولى ثم يمر عبر الفجوة الثانية ليخرج مـن خلال فتحة أخرى متغيرة الموقع على الجدار الأيمن للفجوة الثانية. الشروط الحدية للجدران التي تربط بـين الفجوتين مثبتة عند درجة حرارة ثابتة بينما بقية الجدران للنموذج معزولة. في هذه الدراسة خطوط الجريان،

خطوط درجات الحرارة، معدل درجة الحرارة ومعدل رقم نسلت درست لقيم ريكاردسون Ri تتراوح مـن (0 -10) ، وعدد رينولدز $50 \le Re \le 200$, ارتفاع الجدران الساخنة $0.1 \le H_o \le 0.9$ ومواقع مختلفـة لفتحة الخروج H_{o1} (0.1, 0.5, 0.9) وذلك عند قيم ثابتة لموقع فتحـة الـدخول H_i=0.2 وعـدد برانـدل Pr=0.71. نتائج خطوط الجريان، خطوط درجات الحرارة، معدل رقم نسلت ومعدل درجة الحرارة قورنت مع ما منشورا في [8](Rahman et al. 2007) وأظهرت توافقاً ممتازاً. النتائج العددية أظهرت بان معـدل انتقال الحرارة يعتمد بصورة مهمة على نسبة ارتفـاع الجـدران الـساخنة H_o، قـيم رينولـدز Re وقـيم ريكاردسون Ri. الدراسة أوضحت أن تغير موقع فتحة الخروج ليس له تأثير مهم على معدل انتقال الحرارة وانه بزيادة Ri وRe انتقال الحرارة بالحمل يسود على عملية انتقال الحرارة بالتوصيل.

NOMENCLATURE

D : distance between the two cavities(m)
g : gravitational acceleration (ms^{-2})
H_i : inlet port location
H_o : height of the heated wall
H_{o1} : exit port location
L : length of the cavity
n : normal direction on a plane
N : number of nodes in the element
$\overline{Nu}$: average Nusselt number
Nu_L : local Nusselt number
P : pressure (Nm^{-2})
P : non-dimensional pressure
Pr : Prandtl number
Re : Reynolds number
Ri : Richardson number
s : length of the heated walls
T : temperature (K)
T_h : hot temperature (K)
T_i : inlet temperature (K)
u, v : velocity components (ms^{-1})
U, V : non-dimensional velocity components
W : height of the inflow and outflow openings
x, y : Cartesian coordinates (m)
X, Y : non-dimensional Cartesian coordinates

Greek symbols

α :thermal diffusivity, $k/\rho C_p$ (m^2s^{-1})
β : thermal expansion coefficient (K^{-1})
λ : penalty parameter
θ : non-dimensional temperature
$\theta_{av.}$: average non-dimensional temperature
ν : kinematic viscosity of the fluid (m^2s^{-1})
ρ : density of the fluid (kgm^{-3})
Φ: basis functions

Subscripts

i : residual number
k : node number

INTRODUCTION

Heat transfer in flows in which the influence of forced convection and natural convection are of comparable magnitude (mixed convection flows) occurs frequently in engineering situations. The applications include the design of solar collectors, thermal design of building, air conditioning and cooling of electronic circuit boards etc. Analysis of a mixed convection flow usually requires an understanding of the two limiting regimes. The mixed convection transport is complex due to the interaction of buoyancy force with the shear force (**Rahman et al., 2009**).

There have been many investigators in the past worked on mixed convective flow in ventilated cavities. (**Khanafer et al. 2002**) studied numerically mixed convection heat transfer in open-ended enclosures for three different flow angles of attack. They used a finite element scheme based on the

Galerkin method of weighted residuals. A wide range of pertinent parameters such as Grashof number, Reynolds number, and the aspect ratio are considered. Their results showed that thermal insulation of the cavity can be achieved through the use of high horizontal velocity flow. Various results for the streamlines, isotherms and the heat transfer rates in terms of the average Nusselt number are presented and discussed for different parametric values. (**Rahman et al., 2007**) made a numerical study of mixed convection in a vented enclosure by finite element method. From this study they found that with increase of Reynolds and Richardson numbers the convective heat transfer became predominant over the conduction heat transfer and the rate of heat transfer from the heated wall significantly depended on the position of the inlet port. The higher Nusselt number was observed at very large Prandtl number, and they also derived empirical correlations to express the above relation mathematically. (**Saha et al., 2008**) carried out a numerical analysis to study the performance of mixed convection in a rectangular enclosure. Four different placement configurations of the inlet and outlet openings were considered with a constant flux heat source on the vertical surface. The results indicated that the average Nusselt number and the dimensionless surface temperature on the heat source strongly depended on the positioning of the inlet and outlet openings.

A mixed convection heat transfer in a square cavity with a centered heat conducting horizontal square solid cylinder is solved numerically using finite element method by (**Rahman et al., 2010**). The objective of their work was to identify the influences of the governing parameters, such as Reynolds number, Richardson number, Prandtl number and the inlet and exit port locations of the cavity. Their results showed that Reynolds number has significant effect on the flow field in the pure forced convection and in the pure mixed convection region, but Prandtl number has significant effect on the flow field in the pure mixed convection and in the free convection dominated region. On the other hand, the mentioned parameters have significant effect on the thermal field in the three convective regimes considered. Lastly, the locations of the inlet and outlet port have significant effect on both the flow and thermal fields in the three convective regimes. (**Ghasemi and Aminossadati, 2007**) numerically investigated the cooling performance of electronic devices with an emphasis on the effects of the arrangement and number of electronic components. In this analysis used a two dimensional rectangular enclosure under combined natural and forced convection flow conditions and considered a range of Rayleigh numbers. From the results they found that increasing the Rayleigh number significantly improved enclosure heat transfer process. The arrangement and number of heat sources had a considerable contribution to the cooling performance but they observed that increasing the Rayleigh number reduced this contribution.
(**Saha et al., 2010**) studied numerically the steady state two-dimensional mixed convection problem in a square cavity with the top moving lid and the bottom wall was maintained at constant temperature, while the vertical walls were thermally insulated. (**Theofilis et al., 2004**) studied numerically the viscous linear stability of four classes of incompressible flows inside rectangular containers. In the first class the instability of flow through a rectangular duct, driven by a constant pressure gradient along the axis of the duct was examined (plane Poiseuille flow-PPF). The other classes of flow examined were generated by tangential motion of one wall, in one case in the axial direction of the duct, in another perpendicular to this direction, corresponding respectively to the two-dimensional counterpart to plane Couette flow (PCF) and the classic lid-driven cavity (LDC) flow, and in the fourth case a combination of both the previous tangential wall motions.

(**Rahman et al., 2009**) used the finite element method to solve two-dimensional governing mass, momentum and energy equations for steady state, mixed convection problem inside a vented square cavity. The cavity consisted of adiabatic left, top and bottom walls and heated right vertical wall; but it also contained a heat conducting horizontal square block located somewhere inside the cavity. The results indicated that the block size and location had significant effect on both the flow and thermal fields but the solid-fluid thermal conductivity ratio had insignificant effect on the flow field also indicated that the average Nusselt number at the heated surface, the average temperature of the fluid inside the cavity and the temperature at the center of solid block were strongly dependent on the configurations of the system. (**Manca et al., 2003**) used a numerical analysis of laminar mixed

convection in an open cavity with a heated wall bounded by a horizontally insulated plate. They considered three heating modes in their work, assisting flow, opposing flow and heating from below. Their results reported for Richardson number equal to 0.1 and 100, Re=100 and 1000, and aspect ratio in the range 0.1-1.5 and showed that the maximum temperature values decrease as the Reynolds and Richardson numbers increase and the effect of the ratio of channel height to the cavity height was found to play a significant role on streamline and isotherm patterns for different heating configurations. (**El-Amrani et al., 2007**) performed a numerical investigation to study the solution of natural and mixed convection flows by Galerkin-characteristic method. They found that the Galerkin-characteristic method was feasible and satisfactory for solution.

In the present paper a numerical investigation is accomplished on the mixed convection of air in the double square cavity. The main objective of this work is to examine the effect of exit port locations and the aspect ratio of the hot wall as well as the effect of Reynolds and Richardson numbers on the heat transfer characteristics.

MODEL DESCRIPTION

The model considered here is two cavities connected in series with a constant temperature applied on the opposite walls as shown in **Fig. 1**. The other side walls including top and bottom of the cavities are assumed to be adiabatic. Each cavity has dimensions of ($L \times L$). The inflow opening located on the left vertical wall of the first cavity and it fixed at a height H_i=0.2L from the bottom of the enclosure while the outflow opening located on the right vertical wall of the second cavity and may vary in location at a height H_{o1} from the bottom. The size of the inlet port is the same of the exit port which is equal to W=0.1L. It is assumed that the incoming flow is at a uniform velocity, u_i and at the ambient temperature, T_i.

MATHEMATICAL FORMULATION

Governing Equations

Mixed convection is governed by the differential equations expressing conservation of mass, momentum and energy. The present flow is considered steady, laminar, incompressible and two-dimensional. The viscous dissipation term in the energy equation is neglected. The physical properties of the fluid in the flow model are assumed to be constant except the density variations causing a body force term in the momentum equation. The Boussinesq approximation is invoked for the fluid properties to relative density changes to temperature changes, and to couple in this way the temperature field to the flow field. The governing equations for steady mixed convection flow can be expressed in the dimensionless form (**Rahman et al., 2009**) as.

$$\frac{\partial U}{\partial X}+\frac{\partial V}{\partial Y}=0 \tag{1}$$

$$U\frac{\partial U}{\partial X}+V\frac{\partial U}{\partial Y}=-\frac{\partial P}{\partial X}+\frac{1}{\mathrm{Re}}\left(\frac{\partial^2 U}{\partial X^2}+\frac{\partial^2 U}{\partial Y^2}\right) \tag{2}$$

$$U\frac{\partial V}{\partial X}+V\frac{\partial V}{\partial Y}=-\frac{\partial P}{\partial Y}+\frac{1}{\mathrm{Re}}\left(\frac{\partial^2 V}{\partial X^2}+\frac{\partial^2 V}{\partial Y^2}\right)+Ri\,\theta \tag{3}$$

$$U\frac{\partial \theta}{\partial X}+V\frac{\partial \theta}{\partial Y}=\frac{1}{\mathrm{Re}\,\mathrm{Pr}}\left(\frac{\partial^2 \theta}{\partial X^2}+\frac{\partial^2 \theta}{\partial Y^2}\right) \tag{4}$$

The dimensionless variables are defined as:

$$X=\frac{x}{L},\qquad Y=\frac{y}{L},\qquad U=\frac{u}{u_i},\qquad V=\frac{v}{u_i}$$

$$P=\frac{p}{\rho u_i^2},\qquad \theta=\frac{(T-T_i)}{(T_h-T_i)}$$

Where X and Y are dimensionless coordinates varying along horizontal and vertical directions respectively, U and V are dimensionless velocity components in the X and Y directions respectively, θ is the dimensionless temperature and P is the dimensionless pressure. The non-dimensional numbers seen in the above, *Re*, *Ri* and *Pr are* the Reynolds number, Richardson number and Prandtl number respectively, and are defined as.

$$\mathrm{Re}=\frac{u_i L}{\nu},\qquad Ri=\frac{g\beta(T-T_i)L}{u_i^2},\qquad \mathrm{Pr}=\frac{\nu}{\alpha}$$

Boundary Conditions

The boundary conditions for this analysis are:

- At the inlet: U=1; V=0; θ=0
- At the outlet: $P=0$ (the boundary conditions at the exit port are unknown, so that the values of u, v and T are extrapolated at each iteration step)
- At the heated walls: U=0; V=0; θ=1
- At the rest of the adiabatic walls: U=V=0 , $\frac{\partial\theta}{\partial X}=0$ and $\frac{\partial\theta}{\partial Y}=0$

Heat Transfer Calculations

The local Nusselt number is evaluated (**Rahman et al., 2009**) as:

$$Nu_L=\frac{\partial\theta}{\partial n} \tag{5}$$

where n denotes the normal direction on a plane.
The average Nusselt number

$$\overline{Nu}=\frac{1}{s}\int_0^s Nu_L\,ds \tag{6}$$

where (s) is the length of the heated walls
The bulk average temperature, defined (**Rahman, et al. 2007**) as;

$$\theta_{av.}=\int \theta dV/V \tag{7}$$

where V is the cavities volume.

COMPUTATIONAL PROCEDURE

The code FlexPDE (**Backstrom , 2005**) is used to perform finite element method to analyze the laminar mixed convection heat transfer and air flow in a two cavity connected one with other. It is well known in the numerical solution field that the set of equations above (1-4) may be highly oscillatory or even sometimes undetermined due to inclusion of the pressure term in the momentum equations. In finite element method there is a derived approach with purpose of stabilizing pressure

oscillations and allowing standard grids and elements. This approach enforces the continuity equation and the pressure to give the following, what called penalty approach (**Langtangen, et al. 2002**).

$$\nabla^2 P = \lambda\left(\frac{\partial U}{\partial X}+\frac{\partial V}{\partial Y}\right) \tag{8}$$

Where λ is a parameter that should be chosen either from physical knowledge or by other means (**Langtangen, et al. 2002**). A most convenient value for λ was attained in this study to be $1e5\mu/L^2$. Hence, the continuity eq. (1) is excluded from solution system and replaced be eq. (8).

The system of equations (2), (3), (4) and (8) are solved by using Galerkin finite element method (**Basak et al. 2009**) which the code FlexPDE (**Backstrom, 2005**) is depend it in the solution . Expanding the velocity components *(U, V)*, (*P)* and temperature *(θ)* using basis set $\{\Phi_k\}_{k=1}^{N}$ as,

$$\begin{aligned} U &\approx \sum_{k=1}^{N} U_k \Phi_k(X,Y) \\ V &\approx \sum_{k=1}^{N} V_k \Phi_k(X,Y) \\ P &\approx \sum_{k=1}^{N} P_k \Phi_k(X,Y) \\ \theta &\approx \sum_{k=1}^{N} \theta_k \Phi_k(X,Y) \end{aligned} \tag{9}$$

The Galerkin finite element method yields the following nonlinear residual equations for Eqs. (2), (3), (4) and (8) respectively, at nodes of internal domain Ω:

$$\begin{aligned} R_i^{(1)} &= \sum_{k=1}^{N} U_k \int_\Omega \left[\left(\sum_{k=1}^{N} U_k\Phi_k\right)\frac{\partial\Phi_k}{\partial X}+\left(\sum_{k=1}^{N} V_k\Phi_k\right)\frac{\partial\Phi_k}{\partial Y}\right]\Phi_i dXdY + \sum_{k=1}^{N} P_k\left(\int_\Omega \frac{\partial\Phi_k}{\partial X}\right)\Phi_i dXdY \\ &+ \frac{1}{\mathrm{Re}}\sum_{k=1}^{N} U_k \int_\Omega \left[\frac{\partial\Phi_i}{\partial X}\frac{\partial\Phi_k}{\partial X}+\frac{\partial\Phi_i}{\partial Y}\frac{\partial\Phi_k}{\partial Y}\right]dXdY \end{aligned} \tag{10}$$

$$\begin{aligned} R_i^{(2)} &= \sum_{k=1}^{N} V_k \int_\Omega \left[\left(\sum_{k=1}^{N} U_k\Phi_k\right)\frac{\partial\Phi_k}{\partial X}+\left(\sum_{k=1}^{N} V_k\Phi_k\right)\frac{\partial\Phi_k}{\partial Y}\right]\Phi_i dXdY + \sum_{k=1}^{N} P_k\left(\int_\Omega \frac{\partial\Phi_k}{\partial Y}\right)\Phi_i dXdY \\ &+ \frac{1}{\mathrm{Re}}\sum_{k=1}^{N} V_k \int_\Omega \left[\frac{\partial\Phi_i}{\partial X}\frac{\partial\Phi_k}{\partial X}+\frac{\partial\Phi_i}{\partial Y}\frac{\partial\Phi_k}{\partial Y}\right]dXdY - Ri\int_\Omega\left(\sum_{k=1}^{N}\theta_k\Phi_k\right)\Phi_i dXdY \end{aligned} \tag{11}$$

$$\begin{aligned} R_i^{(3)} &= \sum_{k=1}^{N} \theta_k \int_\Omega \left[\left(\sum_{k=1}^{N} U_k\Phi_k\right)\frac{\partial\Phi_k}{\partial X}+\left(\sum_{k=1}^{N} V_k\Phi_k\right)\frac{\partial\Phi_k}{\partial Y}\right]\Phi_i dXdY + \\ &\frac{1}{\mathrm{Re}\,\mathrm{Pr}}\sum_{k=1}^{N} \theta_k \int_\Omega \left[\frac{\partial\Phi_i}{\partial X}\frac{\partial\Phi_k}{\partial X}+\frac{\partial\Phi_i}{\partial Y}\frac{\partial\Phi_k}{\partial Y}\right]dXdY \end{aligned} \tag{12}$$

$$R_i^{(4)} = \sum_{k=1}^{N} P_k \int_{\Omega} \left[\frac{\partial \Phi_i}{\partial X}\frac{\partial \Phi_k}{\partial X} + \frac{\partial \Phi_i}{\partial Y}\frac{\partial \Phi_k}{\partial Y} \right] dXdY - \lambda \left[\sum_{k=1}^{N} U_k \left(\int_{\Omega} \frac{\partial \Phi_k}{\partial X} \right) \Phi_i dXdY + \sum_{k=1}^{N} V_k \left(\int_{\Omega} \frac{\partial \Phi_k}{\partial Y} \right) \Phi_i dXdY \right] \quad (13)$$

The set of non-linear algebraic equations (10-13) are solved using the code FlexPDE.

Grid Refinement Check

A grid refinement test was performed for a two square cavity connected one with other. The grid dependency is checked together with continuity equation and obtained results showed an exactly validation of the velocity distribution for a grid size obtained by imposing an accuracy of 10^{-4}. This accuracy is a compromised value between the result accuracy and the time consumed in each run. The mesh mode for the present numerical computation for Re=200 and Ri =1 is shown in **Fig. 2a** and the distribution of $\left(\frac{\partial U}{\partial X}+\frac{\partial V}{\partial Y}\right)$ over the domain is presented in **Fig. 2b**.

Code Validation

The present code is extensively validated based on the problem of (**Rahman et al., 2007**). We present here some results obtained by our code in comparison with those reported in Rahman *et al.* for *Re* =100, Ri =1.0 and Pr =0.71. The physical problem studied by Rahman *et al.* was the mixed convection in ventilated cavity with uniform heat flux in right wall and the left, top and bottom walls are insulated. For the same parameters used in (Rahman *et al.*) the average Nusselt number (at the hot wall) comparison is shown in **Table 1** and the average fluid temperature comparison in **Table 2**. **Figure 3** also shows the comparison of the flow and thermal fields at Re=200, Ri =1.0 and Pr=0.71 between the present investigation and (**Rahman et al., 2007**). The present results have an excellent agreement with the results obtained by (**Rahman et al., 2007**). From these comparisons it can be decided that the current code can be used to predict the flow filed for the present problem.

RESULTS AND DISCUSSION

The results are presented for mixed convection inside a double square cavity with opposite heated walls. The inlet port in the first cavity is fixed while the exit port in the second cavity is located at different positions in the cavity walls. The effects of the aspect ratio of the heated walls, the exit port locations, Reynolds number and Richardson numbers on the heat transfer characteristics have been presented. The relative strength of the forced convection over natural convection can be judged on the base of Ri, in the mixed convection. In the case, as *Ri* approaches to unity, the buoyancy effect becomes important. Consequently, the natural convection dominates the mixed convection when *Ri* >1. In the following, several cases related to the different configurations are compared in terms of streamlines, isotherms, and average bulk fluid temperature and Nusselt numbers.

Flow and Thermal Fields Characteristics

Effect of Richardson Number

Fig.4 depicts the influence of Richardson number *Ri* on the flow and temperature fields where *Re*=100, *Pr*=0.71, H_o=0.5 and H_{o1}=0.9. For relatively small values of *Ri* a two circulating cell of different size at the top and bottom of the inlet port is presented in the first cavity while one vortex appears near the bottom of the second cavity due to the effect of the buoyancy. With the increasing the value of *Ri* the size of the circulating cells in the first and second cavities gradually is increased. This is because the buoyancy effects accelerated the fluid near the heated wall causing the recirculation near the bottom of the hot wall.

The corresponding isotherm plots for the above cases are presented in **Fig. 4 (a2)** to **Fig. 4 (c2)**. As shown, the thermal boundary layer decreases in thickness slowly as the *Ri* increases in the first cavity this is because of reducing the fluid density near the heated wall and make a growth of thermal boundary layer . Also it can be seen a large growth of thermal boundary layer as *Ri* increases in the second cavity, this is because the effect of the secondary flow with increasing of *Ri* .

Effect of Reynolds Number

Fig. 5 shows the streamlines and isotherms plot for various values of Reynolds number *Re* at *Ri*=1.0, *Pr*=0.71, H_o=0.5 and H_{o1}=0.9. The recirculation region is dominated at the upper-left corner of the first cavity while it dominate at the bottom part of the second cavity due to the separation phenomena in these parts of flow regions. It can be seen from this figure that the size of the vortex increases with the increasing value of *Re* this is because the increasing of fluid intensity. Corresponding temperature distributions can be seen in **Figures 5 (a2) to 5 (c2)**. It can be seen that increase in *Re* reduces the growth of thermal boundary thickness and it is possible, since at large value of *Re*, the effect of gravitation force becomes negligible.

Effect of Aspect Ratio of Heated Walls

Now the attention is drawn to see the effect of increase of the aspect ratio of hot walls on the flow and temperature distribution in the double square cavity. The streamlines and the isotherms for H_o=0.1, 0.35 and 0.9 are shown respectively in **Fig. 6** while the other parameters are *Re*=100, *Ri* =1.0, *Pr*=0.71 and H_{o1}=0.9. At H_o=0.1 the recirculation region is dominated at the upper part of the enclosure with a small vortex appears in the bottom-left corner of the first cavity. With increases the aspect ratio as shown in **Fig. 6 (b1)** and **6 (c1)** the upper cell is reduced gradually while the other cell is formed in the second cavity and the size of this cell is increased with increasing of H_o due to the effect of separation phenomena. Also **Fig. 6** is illustrated that the intensity of the streamlines is increased with the increasing of aspect ratio. The formation of circulating cell is because of the mixing of the fluid due to buoyancy driven and convective currents. Similarly the isotherms inside the cavities are shown in the **Figures 6 (a2) to 6 (c2)**. It is clear from these figures that the increasing of aspect ratio causing the increasing of the amount of heat transfer to the fluid in the second cavity as the result of this the temperature of the fluid in the second cavity is become more than that in the first cavity due to the dominate of the free convection.

Effect of Exit Port Location

Figure 7 shows the streamlines and isotherms plot for various values of H_{o1}. From this figure it can be seen that the increasing of the intensity of streamlines as the location of the exit port, H_{o1} increases due to the change the direction of the streamlines in the flow and dominate the secondary flow. Similarly the isotherms inside the cavities are shown in the **Figures 7 (a2)**, **7 (b2)** and **7 (c2)** for three different exit port locations H_{o1}=0.2, 0.5 and 0.8 respectively. It is clear from these figures that a small growth of thermal boundary layer near the heated surface for the three different exit port locations. This is because of a small variation of intensity flow with change of exit port location.

Heat Transfer Characteristics

The effect of Reynolds number on the average Nusselt number at the hot walls and the mean bulk temperature of the fluid are displayed as a function of Richardson number for some particular Reynolds number as shown in **Fig. 8** and **Fig. 9** respectively. It is observed from **Fig. 8** that when Ri increases from 0 to 10, the average Nusselt number increases. This behavior results from the onset of thermal instabilities and the probable development of secondary flow due to uniform heating and forced flow, causes rapid mixing from the left to the right inside the enclosure. It is also noting that for the same value of *Ri* the value of average Nusselt number is increased with increasing of *Re* due to the reducing in the growth of the thermal boundary layer near the heated surface and the dominate of forced convection. In the other hand, the average temperature of the

fluid is increased with the increasing the *Ri* but decreases with the increasing *Re*. This behavior is because the increasing of the effect of the buoyancy with the increasing of *Ri* and decreasing *Re*.

Figure 10 illustrates the influence of aspect ratio H_o on the average Nusselt number at the heated walls. Observing that there is no significant change in the value of $\overline{Nu}$ with the increase of Ri at high value of *Ho*. This is because of the increasing of mean bulk temperature of the fluid but for low value of H_o =0.1 the average Nusselt number significant increasing with the increase *Ri*. This is because the boundary layer becomes thick with increasing the aspect ratio

The average temperature of the fluid as a function of Richardson number for different aspect ratio of heated walls H_o =0.1, 0.5 and 0.9 is shown in **Fig. 11**. In this figure it can be seen that for each H_o the average temperature of fluid increases with increasing of *Ri* due to dominate of natural convection and also observed that as aspect ratio increases the average temperature of fluid increases due to increase the amount of heat transfer to the fluid.

The average Nusselt number at the hot walls of the enclosure and the average temperature of fluid as a function of Richardson number for the three different exit port location is shown in **Fig. 12** and **Fig. 13**. It observed that a very little effect of the exit port location on the average Nusselt number and also on the average temperature such that it can be seen that the values of average Nusselt number and temperature are almost equally for the three locations.

CONCLUSION

The following major conclusions may be drawn from the present investigations:

- The average Nusselt number at the heated surfaces is the highest for the lowest value of aspect ratio H_o, but the average temperature of the fluid is the lowest for the lowest value of aspect ratio H_o.
- The exit port location do not has significant effects on the average Nusselt number and on the average temperature of fluid.
- The numerical solution indicates that increasing the value of Re leads to higher heat transfer coefficient and higher intensity of recirculation.
- The increasing of Richardson number improves the heat transfer process.
- The results of the study show that the flow structure and temperature distribution are considerably influenced by the interaction between natural convection and forced convection in the double cavity.

REFERENCES

[1] Backstrom Gunnar,"Fields of Physics by Finite Element Analysis Using FlexPDE," by GB Publishing and Gunnar Backstrom Malmo, Sweden, 2005.

[2] Basak , T, Roy, S., Sharma, P.K. and Pop, I.,"Analysis of Mixed Convection Flows Within A Square Cavity with Uniform and Non-uniform Heating of Bottom Wall",International Journal of Thermal Sciences,Vol. 48, p. 891–912, 2009.

[3] El-Amrani, M. and Seaid, M.,"Numerical Simulation of Natural and Mixed Convection Flows by Galerkin-Characteristic Method", International Journal for Numerical Methods in Fluids, p. 1819–1845, 2007.

[4] Ghasemi, B. and Aminossadati, S.M.,"Numerical Simulation of Mixed Convection in a Rectangular Enclosure with Different Numbers and Arrangement of Discrete Heat Sources", The Arabian Journal for Science and Engineering, Vol.33, No.1B, p.189-207, 2007.

[5] Khalil Khanafer, K., Vafai, K. and Lightstone, M.,"Mixed Convection Heat Transfer in Two-Dimensional Open-Ended Enclosures ", International Journal of Heat and Mass Transfer, Vol. 45, p. 5171–5190, 2002.

[6] Langtangen H.P., Mardal K.A. and Winther R.,"Numerical methods for incompressible viscous flow", Advances in water Resources 25,p. 1125-1146, 2002.

[7] Manca, O., Nardin, S., Khanafer, K., Vaafai, K.,"Effect of Heated Wall Position on Mixed Convection in a Channel with an Open Cavity", Numerical Heat Transfer, Part A, Vol.43, p. 259–282, 2003.

[8] Rahman, M.M. Alim, M.A. Mamun, M.A.H. Chowdhury, M.K. and Islam, A.K.M. S., "Numerical Study of Opposing Mixed Convection in A Vented Enclosure", ARPN Journal of Engineering and Applied Sciences, Vol.2, No.2,p.25-36, 2007.

[9] Rahman, M.M., Alim, M. A. and Saha, S.,"Mixed Convection in A Square Cavity With A Heat-Conducting Horizontal Square Cylinder ", Suranaree J. Sci. Technol. Vol. 17, No. 2, p. 139-153, 2010.

[10] Rahman, M.M., Alim, M.A., Saha, S. and Chowdhury, M.K.,"Effect of The Presence of a Heat Conducting Horizontal Square Block on Mixed Convection Inside a Vented Square Cavity", Nonlinear Analysis: Modelling and Control, Vol. 14, No. 4, p.531–548, 2009.

[11] Rahman, M.M, Elias, Md. and Alim, M. A.,"Mixed Convection Flow in a Rectangular Ventilated Cavity with a Heat Conducting Square Cylinder at The Center", ARPN Journal of Engineering and Applied Sciences, Vol. 4, No. 5,p.20-29, 2009.

[12] Saha, S., Mamun,A.H. Hossain, M.Z. and Sadrul Islam, A.K.M.,"Mixed Convection in an Enclosure with Different Inlet and Exit Configurations", Journal of Applied Fluid Mechanics, Vol.1, No.1,p.78-93, 2008.

[13] Saha, S., Saha, G. and Hasan, N.,"Mixed Convection in a Lid-Driven Cavity with Internal Heat Source", Proceedings of the 13th Annual Paper Meet, p. 1-6, 2010.

[14] Theofilis, V., Duck, P.W. and Owen, J.,"Viscous Linear Stability Analysis of Rectangular Duct and Cavity Flows", J. Fluid Mech, Vol.505, p.249-286, 2004.

Table 1 Effect of Ri on $\overline{Nu}$ for Re=100 and Pr=0.71

Parameter Ri	Present study $\overline{Nu}$	(Rahman et al., 2007) $\overline{Nu}$	Error (%)
0.0	1.710145	1.692	1.072
0.5	1.825962	1.764	3.5126
1.0	1.918679	1.824	5.1907
2.0	2.062255	1.92	7.40911
5.0	2.334851	2.111	10.604

Table 2 Effect of Ri on $\theta_{av.}$ for Re=100 and Pr=0.71

Parameter Ri	Present study $\theta_{av.}$	(Rahman et al., 2007) $\theta_{av.}$	Error (%)
0	0.0564238	0.057377	1.661
0.5	0.0520530	0.052287	0.448
1.0	0.0492715	0.049231	0.082
2.0	0.0460927	0.045866	0.494
5.0	0.0433113	0.042945	0.853

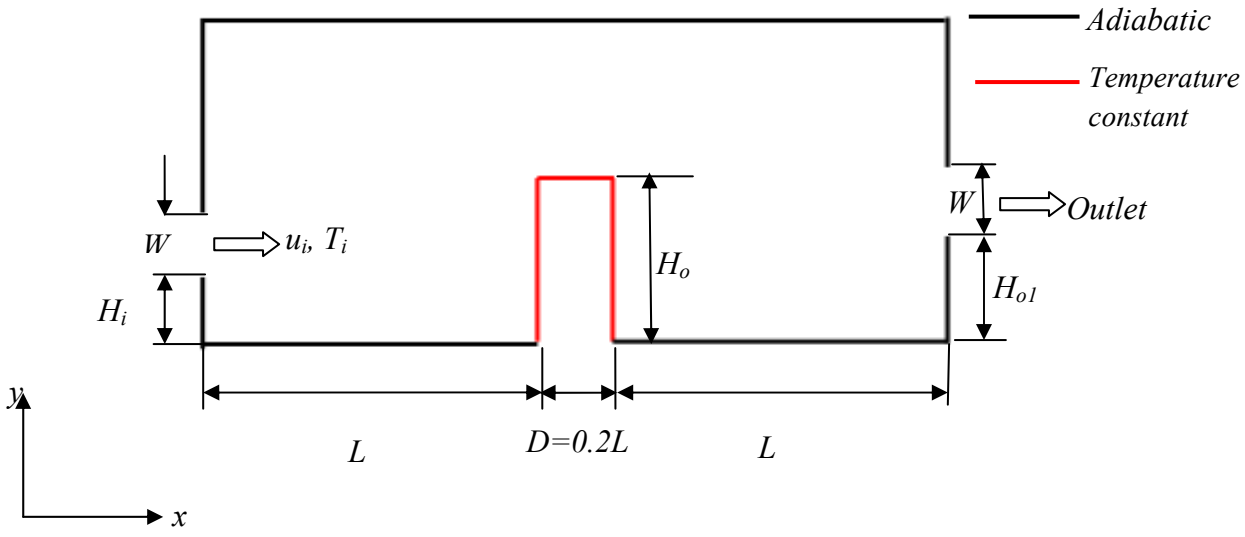

Figure 1 Schematic diagram of the problem

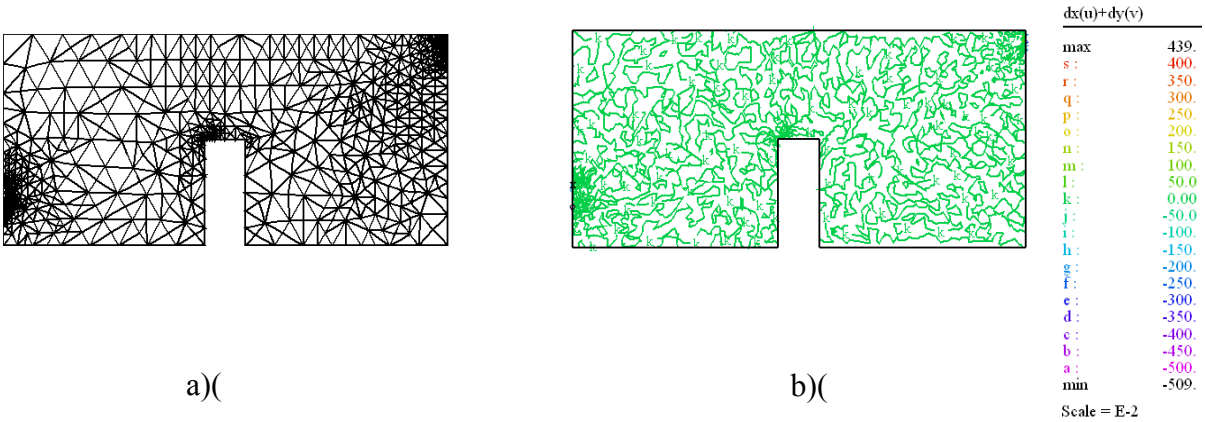

a)(b)(

Figure 2 (a) Grid distribution over the domain (b) Validation of continuity equation

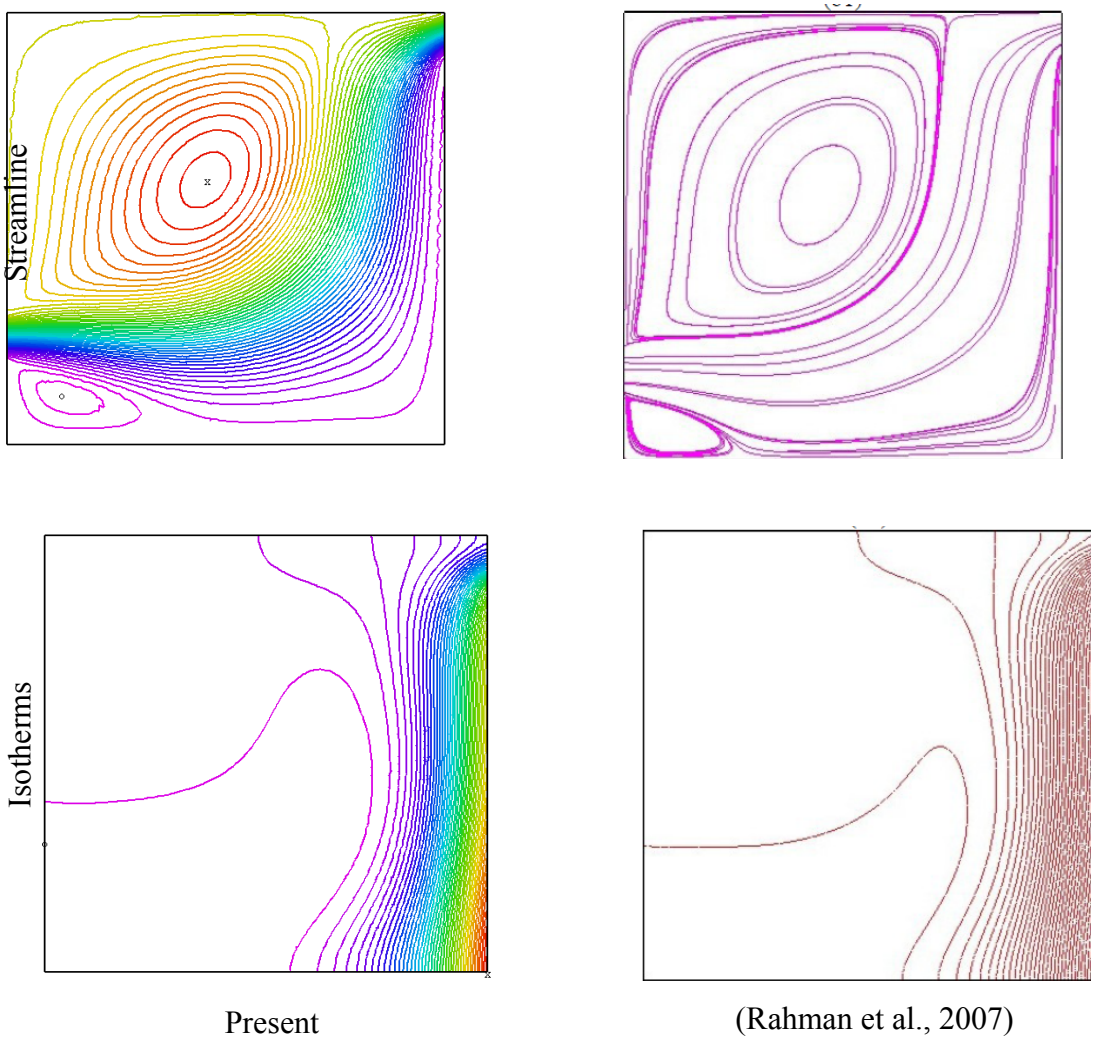

Present (Rahman et al., 2007)

Figure 3 Comparison of streamlines and isotherms for validation at *Re*=200, *Ri*=1 and *Pr*=0.71.

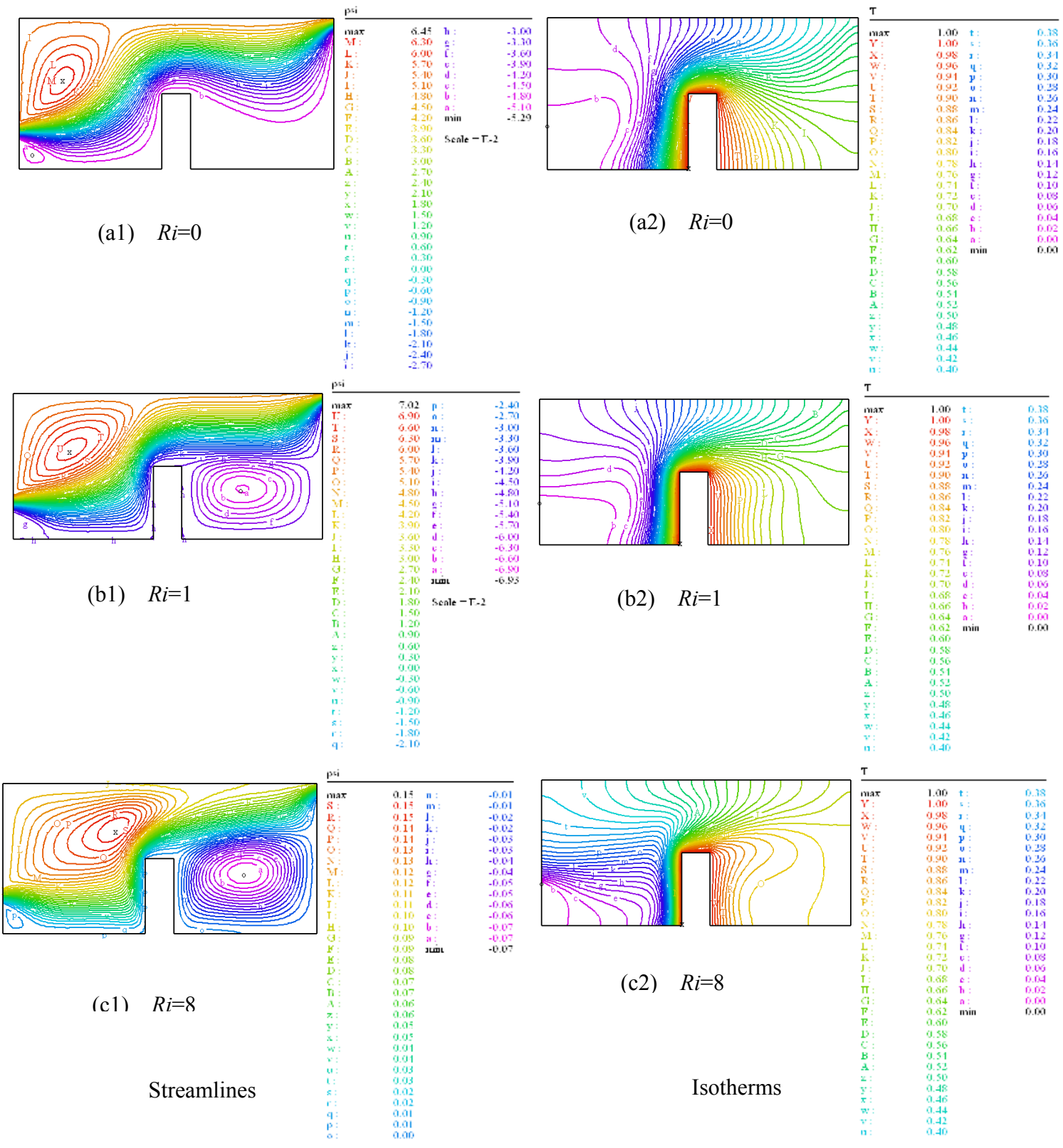

Figure 4 Streamlines and isotherms plot for different Richardson number (*Ri*) at *Re*=100, *Pr*=0.71, H_o=0.5 and H_{o1}=0.9

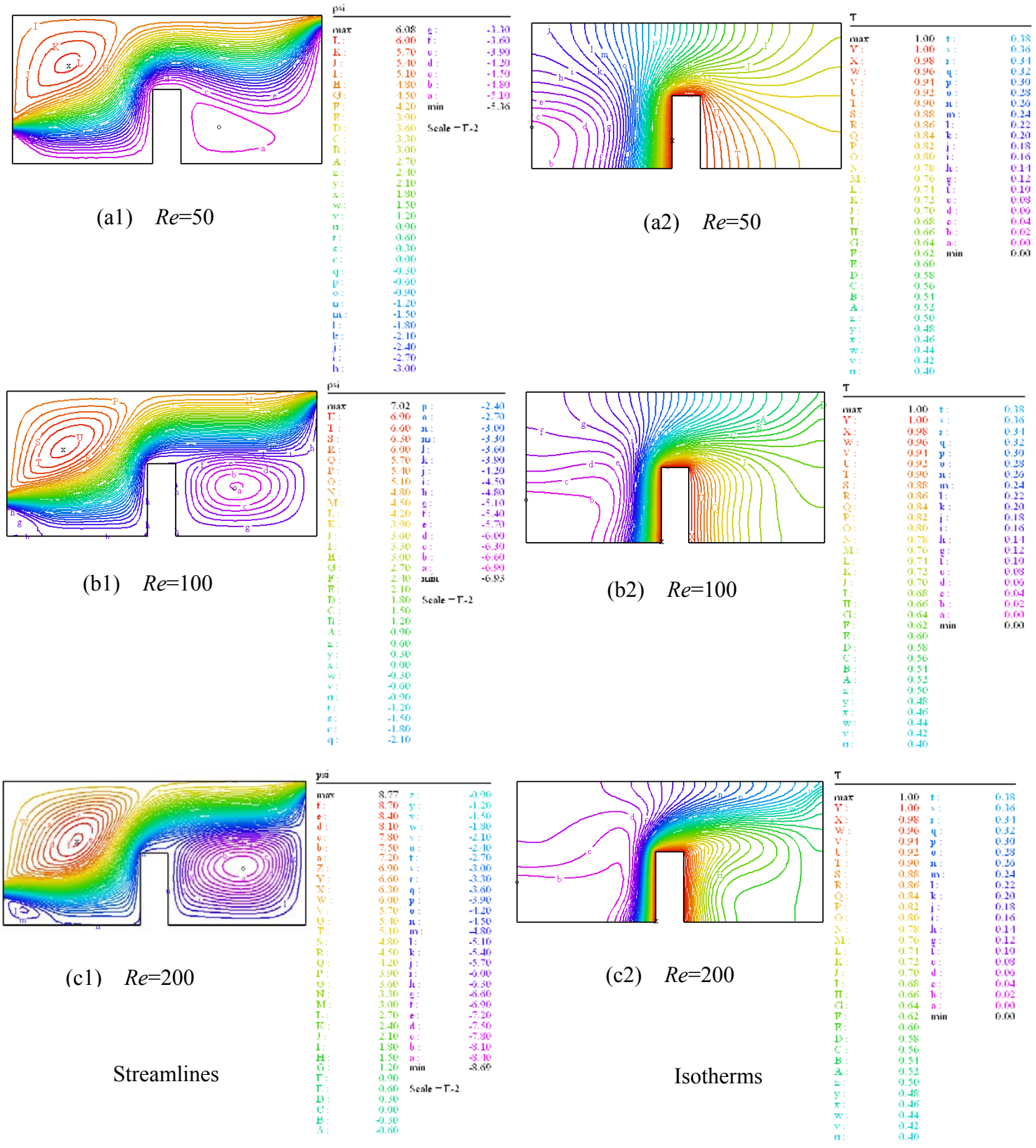

Figure 5 Streamlines and isotherms plot for different Reynolds number (*Re*) at *Ri*=1.0, *Pr*=0.71, H_o=0.5 and H_{o1}=0.9

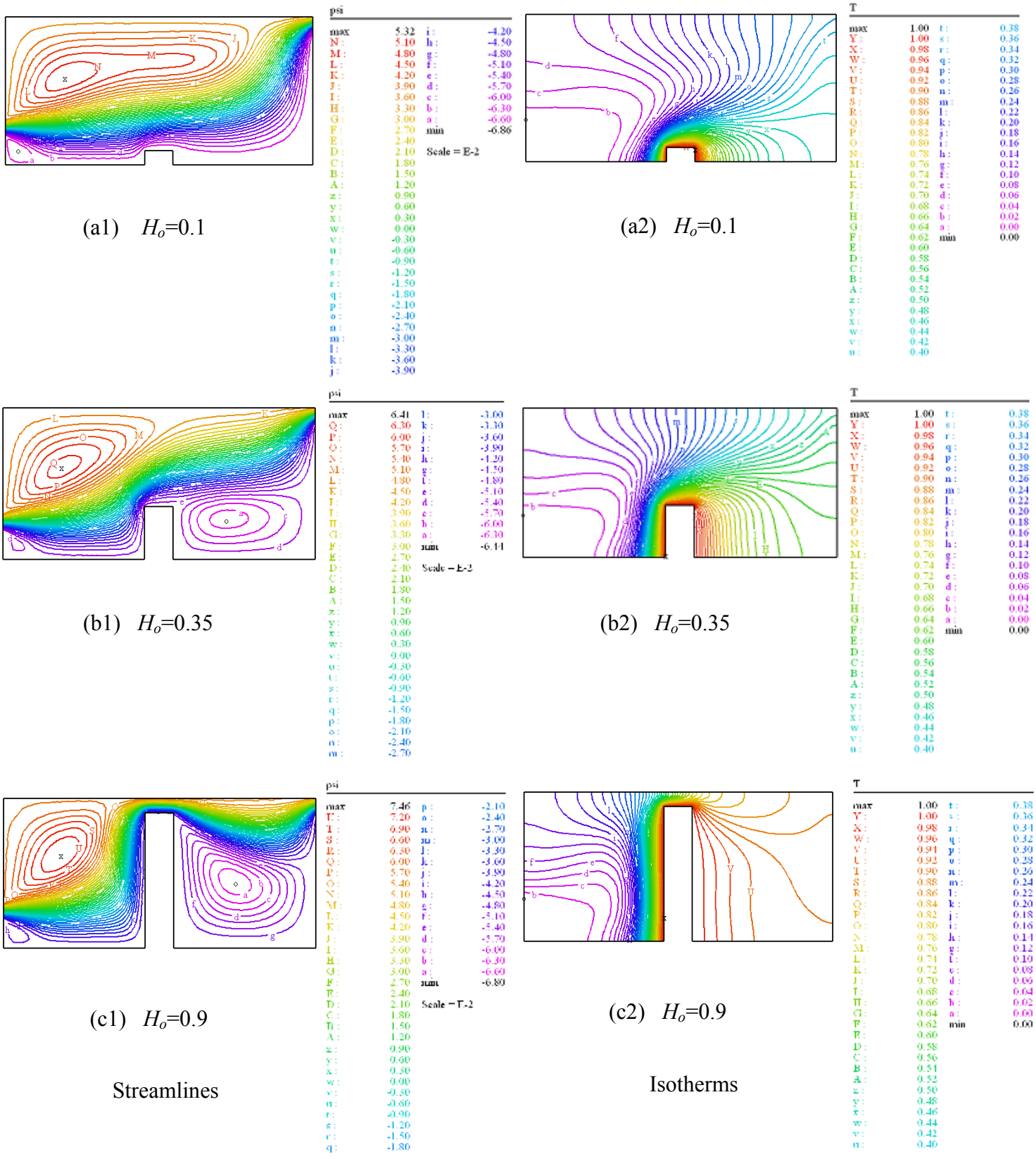

(a1) H_o=0.1 (a2) H_o=0.1

(b1) H_o=0.35 (b2) H_o=0.35

(c1) H_o=0.9 (c2) H_o=0.9

Streamlines Isotherms

Figure 6 Streamlines and isotherms plot for different aspect ratio (H_o) at Re=100, Ri=1.0, Pr=0.71 and H_{o1}=0.9

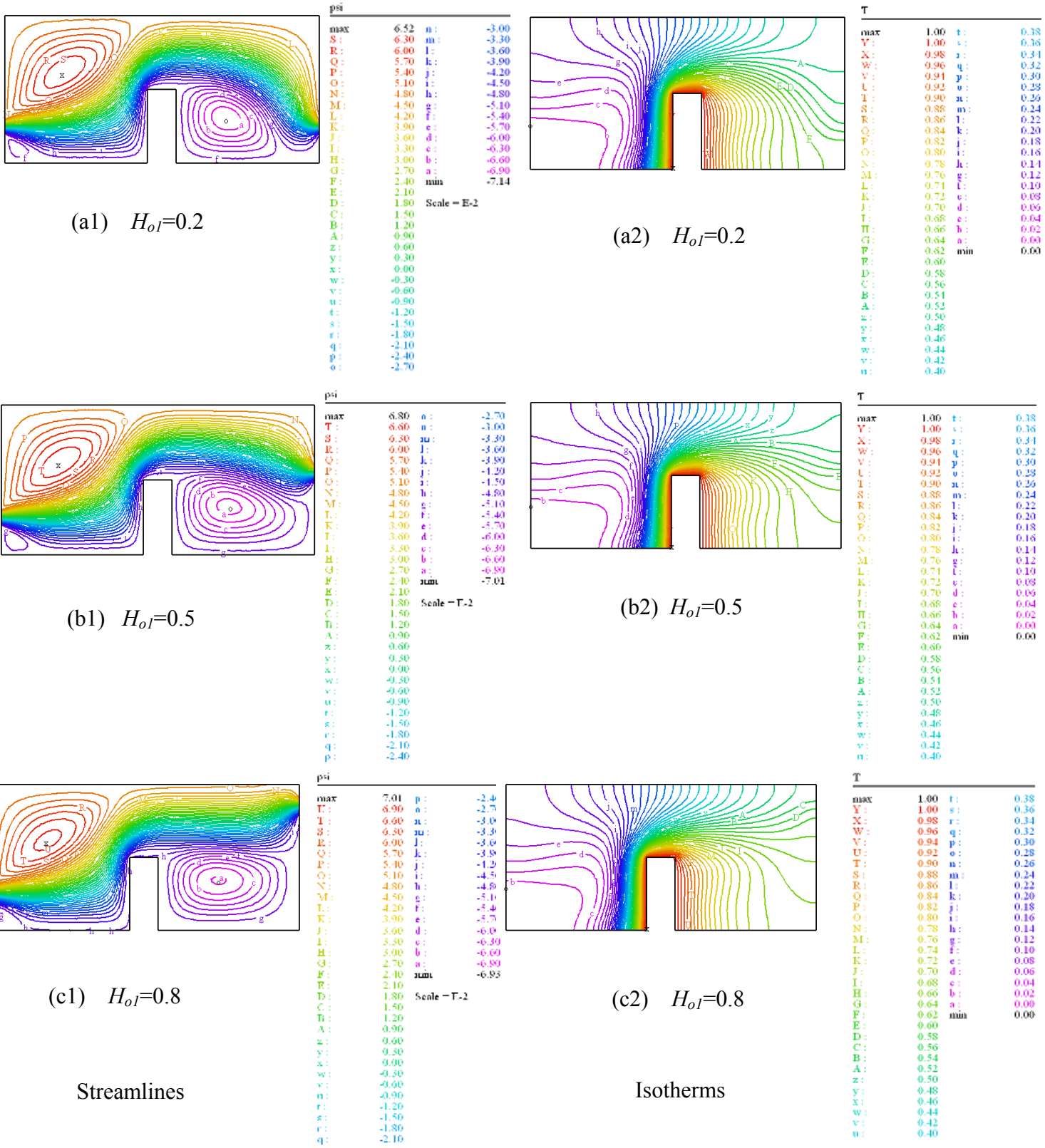

(a1) H_{o1}=0.2

(a2) H_{o1}=0.2

(b1) H_{o1}=0.5

(b2) H_{o1}=0.5

(c1) H_{o1}=0.8

(c2) H_{o1}=0.8

Streamlines

Isotherms

Figure 7 Streamlines and isotherms plot for different exit position (*Ho1*) at *Re*=100, *Ri*=1.0, *Pr*=0.71 and H_o=0.5

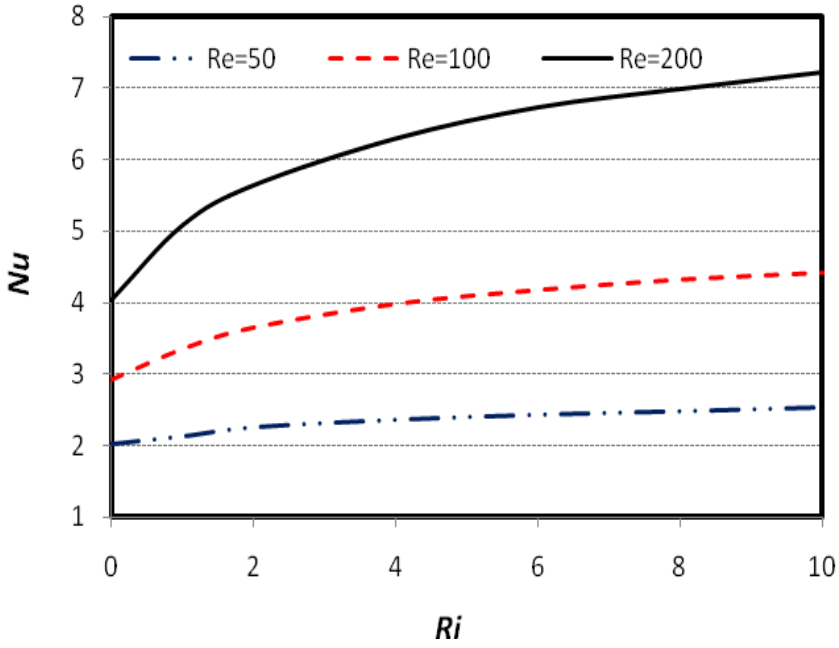

Figure 8 Variation of average Nusselt number with Richardson number

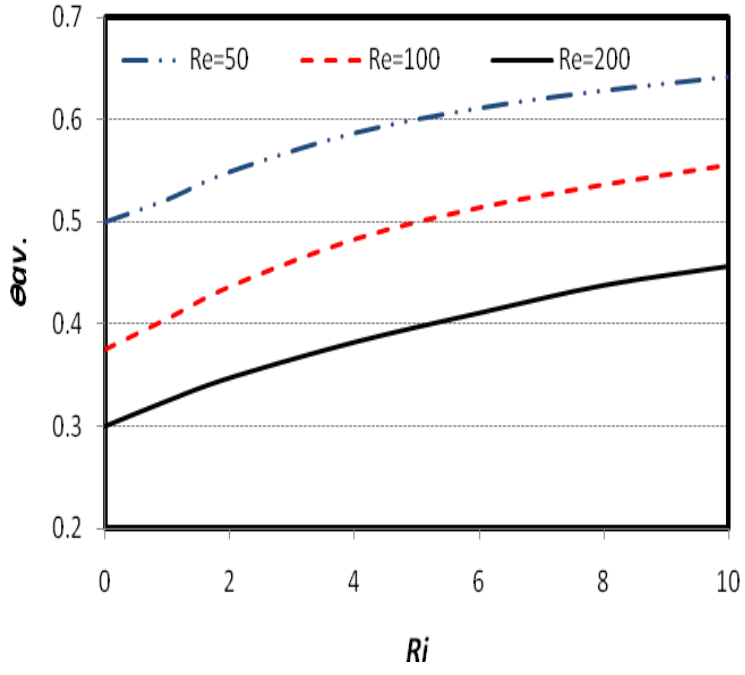

Figure 9 Variation of average temperature as a function of Richardson numbers at different Reynolds numbers.

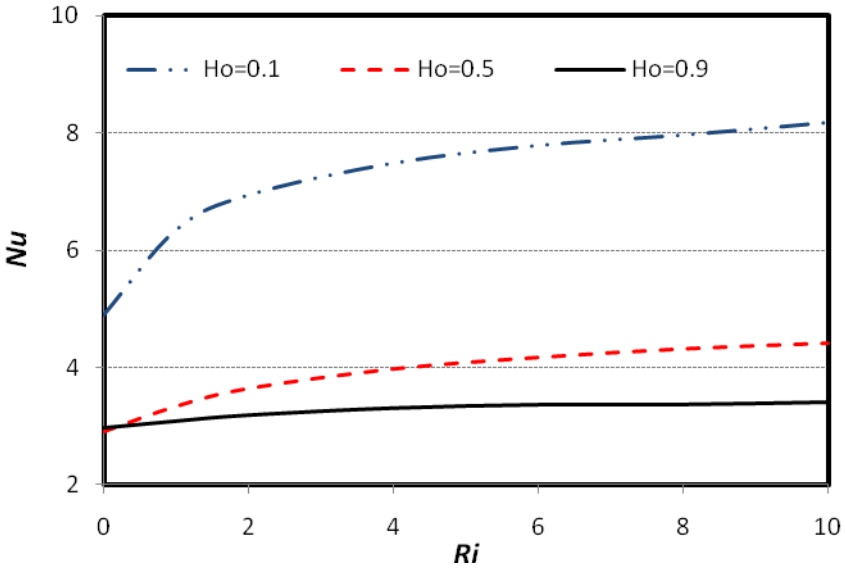

Figure 10 Variation of average Nusselt number as a function of Richardson numbers at aspect ratio of heated walls.

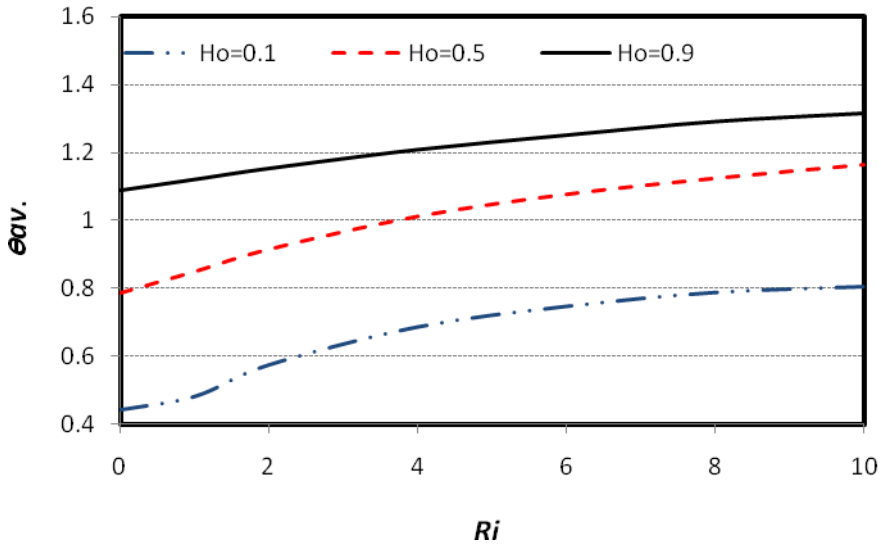

Figure 11 Variation of average temperature as a function of Richardson numbers at aspect ratio of heated walls.

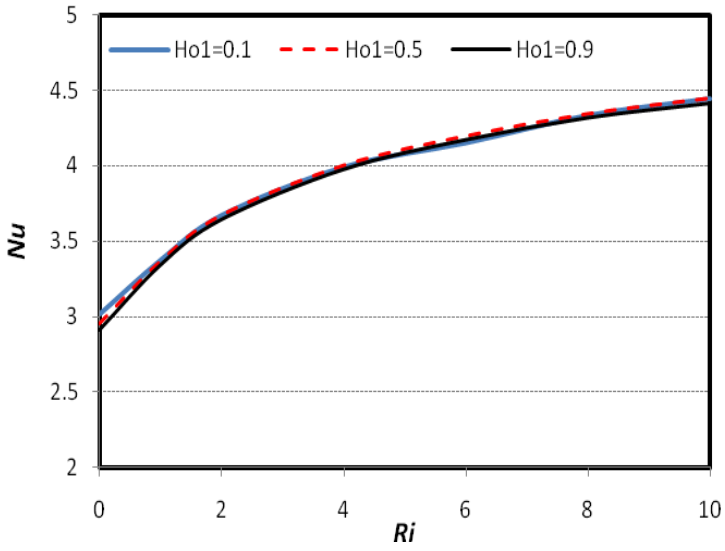

Figure 12 Variation of average Nusselt number as a function of Richardson numbers at different exit port location.

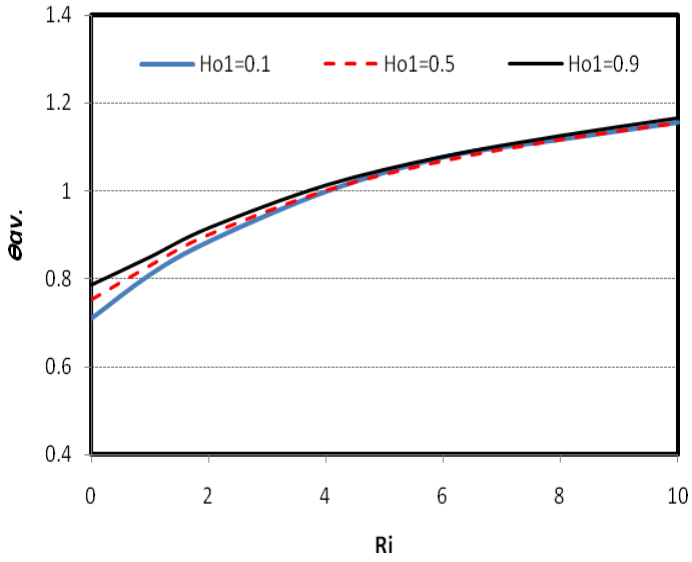

Figure 13 Variation of average temperature as a function of Richardson numbers at different exit port location.